Modern Management Based on Big Data IV
A.J. Tallón-Ballesteros (Ed.)

doi:10.3233/FAIA230210

A Two-Dimensional Numerical Model for Surface Flows with Flexible Vegetation

Chen CHEN[a], Donghua ZHAO[a], Yao WU[a], Yanhao ZHENG[a], Yu DENG[a], Xiangxiang ZHANG[a], Min GAN[b,1] and Xijun LAI[b]
[a] *Shanghai Waterway Engineering Design and Consulting Co., Ltd., Shanghai 200120, China*
[b] *Key Laboratory of Watershed Geography Sciences, Nanjing Institute of Geography & Limnology, Chinese Academy of Sciences, Nanjing 200062, China*

Abstract. According to the demand of large-scale simulation, a numerical simulation model for vegetated flows was developed based on two-dimensional unsteady flow equations. According to the experimental flume results, the influence of aquatic plants on water flow was investigated. The vertical distribution characteristics of the drag coefficient induced by flexible vegetation at different positions of vegetation patches were obtained. The drag coefficients obtained from the experiments were substituted into the model to verify the model's reliability and explore the flow characteristics of open channels with vegetation patches. The results show that: 1) the simulation results of the model are in good agreement with the measured data, which can well simulate the water flow process under the influence of vegetation patches, especially for the far areas with weak three-dimensional effect; 2) The water-blocking effect of the vegetation patch reduces the flow velocity inside the patch and increases the flow velocity in the non-vegetated area on the side, forming a longitudinal shear effect at the edge. The proposed model can support the dynamic analysis of vegetation in rivers, lakes, and estuarine wetland systems.

Keywords. Vegetated flows, open channel, mathematical model, vegetation patches, flexible plant

1. Introduction

Aquatic plant is one of the essential components of the river and lake aquatic ecosystem. Most aquatic plants grow together in communities, forming vegetation zones. The vegetation belt formed by aquatic vegetation has a direct impact on the flow movement of rivers and lakes. Moreover, the changes in the movement structure and turbulence intensity of water flow also affect the circulation of material and energy in the water body. For example, the transport and settlement of sediment or nutrients and the exchange of materials at the water-soil interface can all be influenced [1–3]. The restoration of aquatic ecosystems is mainly based on the revival of aquatic vegetation. Although this method is widely used, the mechanism of ecological and environmental

[1] Min Gan, Key Laboratory of Watershed Geography Sciences, Nanjing Institute of Geography & Limnology, Chinese Academy of Sciences, 200062 Nanjing, China; E-mail: mgan@niglas.ac.cn.
This work was partly supported by the National Natural Science Foundation of China (Grant No.: 42171012).

effects of aquatic vegetation still needs to be further investigated. The impact of aquatic vegetation on water flow is the basis for revealing its ecological and environmental effects [4].

A large number of flume experiments and field observations have been carried out, which provided important data for understanding the impact of vegetation on water flow, sediment, and water quality [5,6]. To better assess and predict the influence of aquatic plants on water flow in the natural environment, the numerical simulation of water flow with vegetation has attracted wide attention. The researches of numerical simulation include the development of the numerical simulation method, revealing the process mechanism of vegetation affecting water flow, and explaining the effects of the plant on the water ecological environment, etc. [7–11]. The 3-D numerical method based on the turbulence model is the primary method for the numerical simulation of flow in open channels with vegetation. However, the two-dimensional model can satisfy the requirements of engineering planning design and its influence study because of its simplicity and practicability. Therefore, the two-dimensional model has been widely used in large-scale calculation and analysis of rivers, lakes, estuaries and wetlands. Due to the differences of plant morphology and characteristics, the magnitude of the influence of various vegetation on water flow movement is significantly different.

Potamogeton Malaianus is a widely distributed species in the rivers and lakes of China [12]. In this paper, based on the flume experiment results of flexible vegetation Potamogeton Malaianus, the additional resistance coefficient of vegetation is obtained. A numerical flow model of wetlands with flexible vegetation was established on the basis of the two-dimensional unsteady flow equations, which provides a scientific tool for understanding the influence of vegetation patches on water flow and dynamic analysis of large-scale river, lake and estuary wetland systems.

2. Materials and Methods

2.1. Numerical Models

- Governing equations

The flow state of the water body can be expressed by using the depth-averaged continuity and motion equations:

$$\frac{\partial \boldsymbol{U}}{\partial t} + \frac{\partial \boldsymbol{F}(\boldsymbol{U})}{\partial x} + \frac{\partial \boldsymbol{G}(\boldsymbol{U})}{\partial y} = \boldsymbol{B}(\boldsymbol{U}) \tag{1}$$

Where t is time; x and y represent the directions in the Cartesian coordinates; $\boldsymbol{U}$ is the vector of the state variables; $\boldsymbol{F}$ and $\boldsymbol{G}$ are the flux vectors along the x and y directions, respectively; $\boldsymbol{B}$ is the vector of the source term. The terms $\boldsymbol{U}$, $\boldsymbol{F}$, $\boldsymbol{G}$, and $\boldsymbol{B}$ have the following expressions:

$$\boldsymbol{U} = (h, hu, hv)^T \tag{2}$$

$$\boldsymbol{F} = (hu, hu^2 + \frac{1}{2} g h^2, huv)^T \tag{3}$$

$$\boldsymbol{G} = (hv, huv, hv^2 + \frac{1}{2}gh^2)^T \tag{4}$$

$$\boldsymbol{B} = \left(0, gh\left(S_{0x} - S_{fx}\right) + S_{veg,x}, gh\left(S_{0y} - S_{fy}\right) + S_{veg,y}\right)^T \tag{5}$$

where h is the water depth; u and v are the depth-averaged velocity along the x and y directions, respectively; T is the symbol of transpose; g is the gravitational acceleration. S_{0x} (S_{fx}) and S_{0y} (S_{fy}) are the bottom (drag) slope terms along the x and y directions, respectively. $S_{veg,x}$ and $S_{veg,y}$ are the additional resistance forces from the vegetables along the x and y directions and have the following expressions:

$$S_{veg,x} = \frac{1}{2}C_p au|u| \tag{6}$$

$$S_{veg,y} = \frac{1}{2}C_p av|v| \tag{7}$$

where C_p is the drag coefficient of the vegetables; a is the vegetable density. C_p is calculated as follows:

$$C_p = \frac{2(gJ - \overline{\Delta u'w'}/\Delta z)}{a(z)u^2} \tag{8}$$

Where J is the hydraulic gradient; $u'w'$ is the Reynolds stress; z is the vertical direction in the Cartesian coordinates; Δz is the vertical distance; $a(z)$ is the vegetable density at z location.

- Numerical solution

In this study, the unstructured grid finite volume method is used to solve the two-dimensional unsteady flow equation [13]. The HLLC (Harten-Lax-van Leer-contact) scheme with high spatial resolution was used to approximate the interface flux. The equation (1) is integrated on any given control volume element, and the Gauss Green formula is used to convert the area integral into a line integral. The original two-dimensional normal flux solution problem is then converted into solving the Riemann problem in a one-dimensional local coordinate system by using the rotational invariance of the convection flux of the control equation [14]. Therefore, only the flux of the normal velocity needs to be calculated to improve the calculation efficiency.

$$\frac{d\boldsymbol{U}}{dt} = -\frac{1}{A}\sum_{j=1}^{m} \boldsymbol{T}(\theta)^{-1}\boldsymbol{F}_j(\overline{\boldsymbol{U}})\, L_j + \overline{\boldsymbol{B}(\overline{\boldsymbol{U}})} \tag{9}$$

where A is the area of the control volume; j is the edge index of the control volume; m is the total number of edges; L_j is the length of j^{th} edge; θ is the intersection angle between x axis and the norm vector (anticlockwise direction of x axis); $\boldsymbol{T}(\theta)$ is the transformation matrix of θ; $\boldsymbol{B}(\overline{\boldsymbol{U}})$ is the comprehensive source terms including the additional vegetation resistance. For more details of the HLLC solution, the readers can refer to reference [14].

- Definite solution condition

To solve the aforementioned equations in a specific condition, the corresponding initial and boundary conditions need to be given simultaneously. The initial conditions are given as follows:

$$\boldsymbol{U}_0 = \left(h|_{t=\boldsymbol{t}_0}, hu|_{t=\boldsymbol{t}_0}, hv|_{t=\boldsymbol{t}_0}\right)^T \tag{10}$$

where the subscript t_0 represent the variable values at the initial condition.

The boundary conditions can be divided into two types which are land boundary and open boundary, respectively. For a given water level (depth) condition, $h(t)|_\Gamma$ is known. According to the known boundary condition on the left-hand state, the unknown boundary condition on the right-hand state can be calculated by the characteristic relation:

$$u_R = u_L + 2\left(\sqrt{gh_L} - \sqrt{gh_R}\right) \tag{11}$$

where subscript R and L represent the variables at the left-hand and the right-hand sides, respectively.

For the land boundary condition, $h_R = h_L$, $u_R = -u_L$, and $v_L = v_R$. The normal flux can be calculated based on the left and right state conditions.

2.2. Physical Experiments

The results from a variable slope flume were used for the validation of the model proposed in this study. As is shown in **Figure 1**, the length and the width of the flume are 38.00 m and 0.80 m, respectively. The vegetation belt is located 10.00 m away from the front of the flume. Its length is 1.60 m and its width is 0.40 m. The height of the vegetation canopy is about 0.14 m. More details of the flume experiments can be found in reference [15].

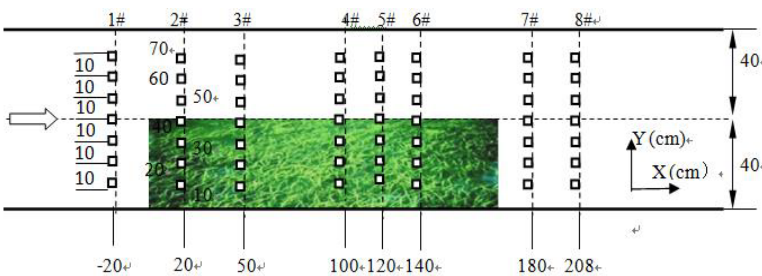

Figure 1. Location of the vegetable patch and the distributions of the observation sections.

3. Results & Discussion

According to the experimental results, the vegetation resistance coefficient can be calculated from the measured U_i, $-\overline{u'w_i'}$, and the hydraulic gradient. The vertical distribution of C_p at different cross sections is shown in **Figure 2**. In general, the resistance coefficient above the vegetation canopy is between 1.4-4.0. When the relative water depth is less than 0.27, the drag coefficient decreases with the increase of water depth. However, when the relative water depth is greater than 0.80, the drag coefficient increases with the increase of water depth. The vertical distribution of the additional resistance coefficient varies greatly due to the swing of aquatic plants. Therefore, the vertical average values were used in the two-dimensional model of this study.

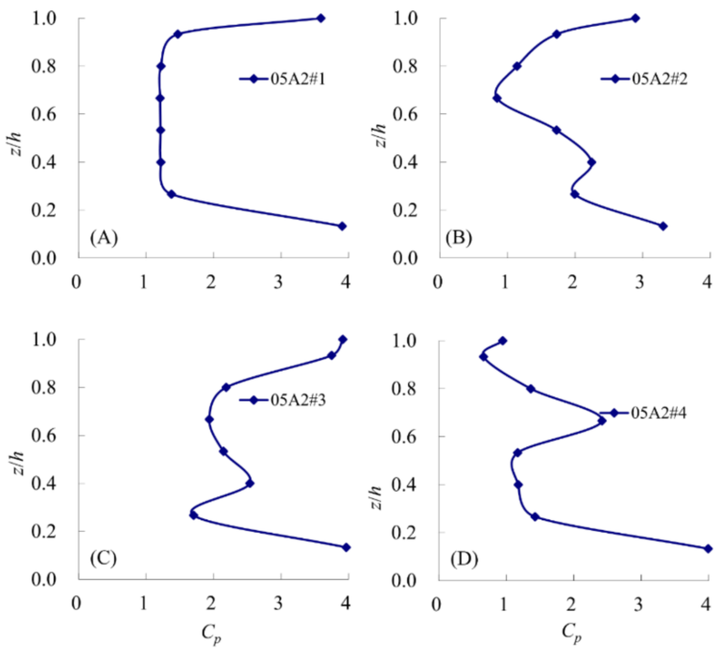

Figure 2. The vertical distribution of C_p at different cross sections.

Based on the size information of the flume, the mesh size of the two-dimensional model was specified as 0.025 m×0.100 m. The flow velocity at the water inlet was set as 0.5 cm/s. The water level at the inlet was set as 0.30 m which is the same as the actual water depth under the experimental condition. The slope of the flume is 0.005, while the manning roughness coefficient is 0.016.

Taking sections 2#, 3#, 4# and 6# as examples, the simulated current velocity was compared with the measurements. Seven average velocities can be obtained for one cross-section when the vertical velocity is averaged (**Figure 1**). **Figure 3** shows the comparison of the model results and the measurements. Overall, the model results get closer to the measurements along the water flow direction. When the water just enters the vegetation area, its three-dimensional flow characteristics are significant because of the mutual influence of the water flow and the vegetation patch. With the downward flow of the water, the flow movement is adjusted to be more stable, and its two-dimensional flow characteristics become more prominent. **Figure 3** illustrates that the flow with flexible vegetation can be simulated by increasing the additional resistance coefficient, and the model developed in this study can be used to analyze the water flow with a weak three-dimensional effect.

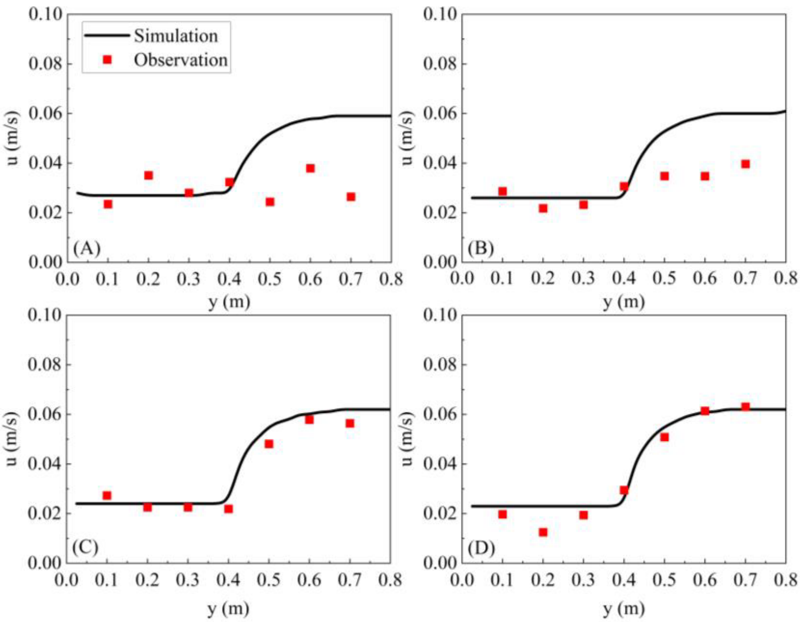

Figure 3. Comparison of the observed and simulated current velocities at sections 2# (A), 3# (B), 4# (C), and 6# (D).

The streamline and the current velocity field from the model results are shown in **Figure 4**. At 0.20 m upstream of the vegetation patch (#2 cross-section), the phenomenon of the flow around the vegetation patch appears due to the water-blocking effect. The flow velocity at the vegetation and non-vegetation areas are weakened and enhanced, respectively. In addition, the flow velocity in the vegetation area decreases along its flow direction because of the water-blocking effect. However, the flow velocity becomes larger when the non-vegetation site is farther away from the vegetation area. The flow velocity is still at a low-velocity state in the areas near the downstream of the vegetation area, indicating that the flow velocity needs to flow some distances to recover to the state without the influence of the vegetation patch.

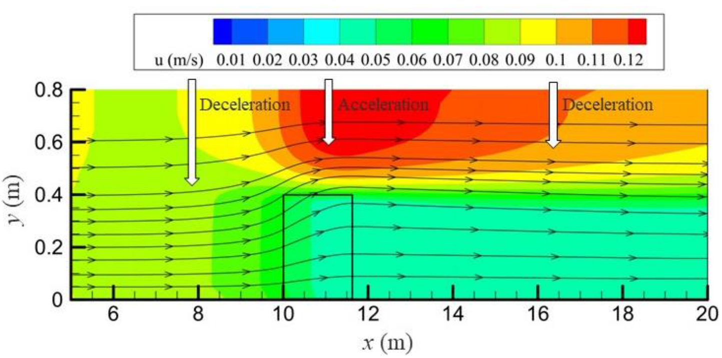

Figure 4. The flow line and current velocity field from the model results.

4. Conclusions

In this paper, a two-dimensional unsteady flow model with the consideration of vegetation is established. The model is validated and calculated by considering the influence of vegetation patches on open channel flow based on the experimental flume results. The common aquatic plant *Potamogeton Malaianus* in the river and lake waters of China was used as the object to obtain the experimental data.

The results show that: 1) The model simulation results are in good agreement with the measured data and can simulate the flow process influenced by vegetation patches, especially in the remote area where the three-dimensional effect is weak; 2) The water-blocking action of the vegetation patches reduces the flow velocity inside the vegetation patches and increases the flow velocity in the vegetation-free areas, resulting in longitudinal shear at the edges.

References

[1] Nepf H, Koch E. Vertical secondary flows in submersed plant-like arrays. Limnology and Oceanography. 1999; 44(4): 1072-1080.
[2] Chen Y, Kao S. Velocity distribution in open channels with submerged aquatic plant. Hydrological Processes. 2011; 25(13): 2009-2017.
[3] Gambi M, Nowell A, Jumars P. Flume observations on flow dynamics in zostera marina (eelgrass) beds. Marine Ecology Progress Series. 1990; 61(1/2): 159-169.
[4] Fagherazzi S, Kirwan M, Mudd S, Guntenspergen G, Temmerman S. Numerical models of salt marsh evolution: ecological, geomorphic, and climatic factors. Reviews of Geophysics. 2012; 50(1): RG1002.
[5] Yamasaki T, Jiang B, Janzen J, Nepf H. Feedback between vegetation, flow, and deposition: a study of artificial vegetation patch development. Journal of Hydrology. 2021; 598: 126232.
[6] Zhang Y, Lai X, Ma J, Zhang Q, Yu R, Yao X, Deng H. Field study on flow structures within aquatic vegetation under combined currents and small‐scale waves. Hydrological Processes. 2021; 35(4): e14121.
[7] Li C, Xie J. Numerical modeling of free surface flow over submerged and highly flexible vegetation. Advances in Water Resources. 2011; 34(4): 468-477.
[8] Lu J, Dai H. Numerical modeling of pollution transport in flexible vegetation. Applied Mathematical Modelling. 2018; 64: 93-105.
[9] Stoesser T, Wilson C, Bates P, Dittrich A. Application of a 3D numerical model to a river with vegetated floodplains. Journal of Hydroinformatics. 2003; 5(2): 99-112.
[10] Huai W, Zhang J, Katul G, Cheng Y, Tang X, Wang W. The structure of turbulent flow through submerged flexible vegetation. Journal of Hydrodynamics. 2019; 31(2): 274-292.
[11] Pu J, Ricardo A, Ferreira R. A Review on hydrodynamics of free surface flows in emergent vegetated channels. Water. 2020; 12(4): 1218.
[12] Dong B, Zhou Y, Jeppesen E, Qin B, Shi K. Six decades of field observations reveal how anthropogenic pressure changes the coverage and community of submerged aquatic vegetation in a eutrophic lake. Science of The Total Environment. 2022; 842: 156878.
[13] Zhao D, Shen H, Tabios G, Lai J, Tan W. Finite‐volume two‐dimensional unsteady‐flow model for river basins. Journal of Hydraulic Engineering. 1994; 120 (7): 863‐883.
[14] Lai X, Jiang J, Liang Q, Huang Q. Large-scale hydrodynamic modeling of the middle Yangtze river basin with complex river–lake interactions. Journal of Hydrology. 2013; 492: 228-243.
[15] Zhang Y, Lai X, Jiang J. The impact of plant morphology on flow structure: comparative analysis of two types of submerged flexible macrophyte. Hydrological Sciences Journal. 2016; 61(12): 2226-2236.